267

The Dipole Observed in the *COBE* DMR Four-Year Data

C. H. Lineweaver[1,2], L. Tenorio[3], G. F. Smoot[4], P. Keegstra[5], A. J. Banday[5] & P. Lubin[6]

Kogut, Hinshaw

Draft printed January 18, 1996

ABSTRACT

The largest anisotropy in the cosmic microwave background (CMB) is the ≈ 3 mK dipole assumed to be due to our velocity with respect to the CMB. Using the four year data set from all six channels of the COBE Differential Microwave Radiometers (DMR), we obtain a best-fit dipole amplitude $3.357 \pm 0.001 \pm 0.023$ mK in the direction $(\ell, b) = (264^{\circ}.33 \pm 0^{\circ}.04 \pm 0^{\circ}.13, +48^{\circ}.05 \pm 0^{\circ}.02 \pm 0^{\circ}.09)$, where the first uncertainties are statistical and the second include calibration and combined systematic uncertainties. This measurement is consistent with previous DMR and FIRAS results.

1. Introduction

The Sun's motion with respect to the cosmic microwave background (CMB) is believed to be responsible for the largest anisotropy seen in the COBE DMR maps: the ≈ 3 mK dipole in the direction of the constellation Leo. A measurement of this Doppler dipole thus tells us the Sun's velocity with respect to the rest frame of the CMB. The accuracy of the determination of this dipole has been increasing steadily since its first detections (for a review see Partridge 1995). A high precision measurement of the amplitude serves as an independent calibrator for ground, balloon and future satellite anisotropy experiments. The CMB dipole is also used to calibrate bulk flow observations which yield independent but much less precise dipole values. In addition, anisotropy measurements in other background radiations will be made in the future and an eventual test of the Doppler origin of the CMB dipole will be facilitated by a CMB dipole of

---

[1] Observatoire de Strasbourg, 67000 Strasbourg, France.

[2] e-mail: charley@cdsxb6.u-strasbg.fr

[3] Universidad Carlos III, Madrid, Spain.

[4] LBL, SSL & CfPA, Building 50-205, University of California, Berkeley CA 94720.

[5] Hughes STX Corporation, LASP, Code 685, NASA/GSFC, Greenbelt MD 20771.

[6] UCSB Physics Department, Santa Barbara, CA 93106.

maximum precision (Lineweaver *et al.* 1995). The goal of this paper is to use the DMR four-year data to determine as precisely as possible the direction and the amplitude of the observed dipole.

In Section 2 we discuss the data analysis and in Section 3 we present our results. In Section 4 we discuss contamination from Galactic emission as well as other factors contributing to the error budget. We then discuss and compare our results to FIRAS (Fixsen *et al.* 1994, Fixsen *et al.* 1996) and other reported DMR dipole results (Kogut *et al.* 1993, Bennett *et al.* 1994, Bennett *et al.* 1996).

2. Data Analysis

The DMR radiometers consist of pairs of antennas separated by 60°, each pointing 30° from the satellite spin axis. There are 2 independent channels at each of the 3 frequencies 31.5, 53 and 90 GHz. Each half-second measurement in a given channel is the difference in temperature observed by the two antennas. The four year DMR data set and its systematic errors and calibration procedures are described in Kogut *et al.* (1996). The data used for that analysis are the same used in this paper. We base our results on all six DMR channels since the less sensitive 31 GHz channels provide useful information on the frequency dependence of Galactic contamination.

We use three methods to obtain the CMB dipole amplitude and direction. These methods differ in the form of the input data but all of them are least-squares fits of the data to the coefficients of a spherical harmonic decomposition of the sky: $T(\theta, \phi) = \sum_{\ell m} a_{\ell m} Y_{\ell m}(\theta, \phi)$, where the $Y_{\ell m}$ are real-valued spherical harmonics as described in Smoot *et al.* (1991) and the dipole vector is $\vec{D} = \sqrt{3/4\pi}(-a_{1,1}, -a_{-1,1}, a_{1,0})$. To obtain the dipole we minimize the three quantities:

$$\sum_{i} [T_i - \sum_{\ell=0}^{\ell_{max}} \sum_{m=-\ell}^{+\ell} a_{\ell m} Y_{\ell m}(i)]^2/\sigma_i^2 \tag{1}$$

$$\sum_{t} [\Delta T(t) - \sum_{\ell=0}^{\ell_{max}} \sum_{m=-\ell}^{+\ell} a_{\ell m} (Y_{\ell m}(t_+) - Y_{\ell m}(t_-))]^2/\sigma_t^2 \tag{2}$$

$$\sum_{i,j>i} [\Delta T_{ij} - \sum_{\ell=0}^{\ell_{max}} \sum_{m=-\ell}^{+\ell} a_{\ell m} (Y_{\ell m}(i) - Y_{\ell m}(j))]^2/\sigma_{ij}^2 \tag{3}$$

where T_i is a pixelized DMR temperature map, $\Delta T(t)$ is a single DMR differential measurement and $Y_{\ell m}(t_+)$ and $Y_{\ell m}(t_-)$ are the spherical harmonics evaluated in the pointing directions of the DMR "+" and "–" horns respectively, at time t. The pixel-pair data, ΔT_{ij}, is the average over all single measurements $\Delta T(t)$ where the antennas are pointing at pixels i and j. The denominators are the variances of the input data. Thus, with method 1, the sum is over all map pixels, with method 2, the sum is over all the time-ordered data (with no pixelization) and in method 3 the sum is over all pixel-pairs. The three methods are consistent and agree to within the relatively small noise-only error bars for each channel. We use the difference between the non-pixelized method and the mean of the two pixelized methods to estimate the data pixelization correction. We adopt the mean of these three methods and include the difference in the combined systematic uncertainty. We correct for beam smoothing by multiplying the amplitude by the factor 1.005 (Wright *et al.* 1993). We use the frequency and Galactic latitude cut dependence of the dipole solutions to estimate the effect of Galactic contamination.

3. Results

The dipole amplitude and direction results from each channel and each Galactic plane cut are shown in Figure 1. Table 1 lists the weighted average of the 10° and 15° Galactic cut results and the uncertainties for each channel. We discuss this choice in the next section. Taking the weighted average of all six channels we obtain a best-fit dipole amplitude $3.357 \pm 0.001 \pm 0.023$ mK in the direction $(\ell, b) = (264^\circ.33 \pm 0^\circ.04 \pm 0^\circ.13,\ +48^\circ.05 \pm 0^\circ.02 \pm 0^\circ.09)$, where the first uncertainties are statistical and the second are estimations of the combined systematics. In celestial coordinates the direction is $(\alpha, \delta) = (11^h\ 12^m\ 0^s \pm 17^s, -7^\circ.23 \pm 0^\circ.07)$ (J2000). The uncertainty in the dipole amplitude is dominated by the absolute calibration of the DMR instrument (Kogut *et al.* 1996a). The calibration uncertainty plays no role in the directional uncertainty for the same reason that the directions of vectors $\vec{x}$ and $a\vec{x}$ (where a is any positive constant) are the same. The uncertainty in the direction is dominated by the combined systematic effects discussed in the next section.

Under the assumption that the Doppler effect is responsible for the entire CMB dipole, the velocity of the Sun with respect to the rest frame of the CMB is 368.9 ± 2.5 km/s, which corresponds to the dimensionless velocity $\beta = 1.231 \pm 0.008 \times 10^{-3}$. The associated rms Doppler quadrupole[7] is $Q_{rms} = 1.23 \pm 0.02\ \mu$K with components $[Q_1, Q_2, Q_3, Q_4, Q_5] = [0.91 \pm 0.02, -0.20 \pm 0.01, -2.05 \pm 0.03, -0.91 \pm 0.02, 0.18 \pm 0.01]\mu$K.

$(1.2 \times 10^{-3})^2 \times \frac{1}{2} = 0.7 \times 10^{-6}$

4. Analysis of Galactic Plane Cuts

4.1. Galactic Contamination

---

[7] $Q^2_{rms} = \frac{4}{15}[\frac{3}{4}Q_1^2 + Q_2^2 + Q_3^2 + Q_4^2 + Q_5^2]$ where the components are defined by $T_o \frac{\beta^2}{2}(2cos^2\theta - 1) = Q_1(3sin^2 b - 1)/2 + Q_2 sin2b\, cos\ell + Q_3 sin2b\, sin\ell + Q_4 cos^2 b\, cos2\ell + Q_5 cos^2 b\, sin2\ell$, where T_o is the mean CMB temperature and θ is the angle between the dipole direction and the direction of observation: (ℓ, b).

We estimate the influence of Galactic emission on the measurement, by solving for the dipoles in equations (1), (2), and (3) for a series of Galactic plane latitude cuts. Figure 1 displays the frequency and Galactic latitude cut dependence of the dipole amplitudes and directions. In the top panel, for each channel, the results for six Galactic plane cuts are shown. The bottom panel displays the directions of the same dipole solutions and shows the obvious effect of low latitude Galactic emission. Solutions for the dipole where no effort has been made to eliminate Galactic emission (i.e., 0° Galactic cuts) are labeled with the channel names "53A", "53B", "90A" and "90B". The 31 GHz labels indicate the 5° cut solutions since their 0° cut solutions are off the plot at longitude $\approx 271^\circ$. The Galactic Center is $\approx 94^\circ$ away in the direction indicated by the arrow. Since the Galactic Center is brighter than the Galactic Anti-Center, Galactic emission produces a dipole which pulls the solutions towards it. This is easily seen from the locations of the 0° and 5° cut solutions relative to the cluster of higher cut results on the right.

Since the Galactic dipole vector is nearly orthogonal to the CMB dipole vector, it is almost maximally effective in influencing the CMB dipole direction and almost minimally effective in influencing the CMB dipole amplitude. We can get a rough estimate of the Galactic dipoles by noting that the 0° cut solutions for 31, 53 and 90 GHz are displaced from the direction of our best-fit CMB dipole by angles $\alpha_\nu \approx (5^\circ,\ 1^\circ,\ 0^\circ.5)$ respectively. Thus the ratios of the Galactic dipoles to the CMB dipole are $\frac{D_{Gal,\nu}}{D_{CMB}} \approx sin(\alpha_\nu) \approx (9\%, 2\%, 1\%)$. In Figure 1, the general increase of the dipole amplitudes seen in the top panel as the Galactic cut increases from 0° to 5° to 10° can be explained by the fact that the Galactic dipole vector contains a component in the opposite direction to the CMB dipole ($94^\circ > 90^\circ$) and thus reduces the total dipole in the maps. A rough estimate of this effect on the dipole solutions D is in good agreement with the plot: $\Delta D_\nu \sim sin(4^\circ)\ sin(\alpha_\nu) D \sim (20\,\mu\mathrm{K},\ 5\,\mu\mathrm{K},\ 2\,\mu\mathrm{K})$ for 31, 53 and 90 GHz respectively.

Figure 1 clearly shows the influence of the Galaxy for the 0° and 5° cuts as well as the relative agreement of the independent channel results for both amplitude and direction. It is also apparent that to first approximation a 10° cut is sufficient to remove the effect of the Galaxy on the direction of the best-fit dipole; increases of the cut from 10° to 15° and so on, do not push the directions away from the Galactic center or in any other particular direction. The results tend to cluster together. The directional precision of the various channels and Galactic cuts is seen to be $\sim 0^\circ.3$ and it is perhaps reassuring to note that at the bottom and the top of the cluster are the least sensitive 31A and 31B solutions.

Figure 2 is an attempt to minimize the confusion of taking a closer look at the cluster of points in Figure 1. It analyzes the directional changes of the dipoles in the bottom panel of Figure 1. For example consider the 31A results. The angular difference between the 5° and 10° cut solutions is a vector of length $\approx 1^\circ$ starting from the 5° cut on the left and extending to the 10° cut on the right. Averaging this vector with the analogous vector from 31B, we obtain the long thin line that runs across most of the lower panel in Figure 2. The size of this angular deviation ($\approx 1^\circ$), is plotted as the triangular point in the 5-10 bin of the top panel. An analogous procedure was followed for all channels and Galactic cuts. The channel-averaged results for 31.5, 53 and 90 GHz are represented respectively by triangles, squares and circles in the top panel and thin, medium and thick lines in the bottom panel. Figure 2 is thus a spectral analysis of the angular deviations from one Galactic plane cut to another. To compare directions, the three vectors in a given bin originate at the same point.

Galactic emission significant enough to affect the dipole results will tend to pull the three channels in approximately the same direction and favor a spectral behavior typical of synchrotron or free-free emission. In the top panel, the two reference lines originating on the 31 GHz point in the 0-5 and 5-10 bins indicate this expected spectral behavior for synchrotron radiation (thin) and free-free emission (thick). The results in the 0-5 and 5-10 bins are obviously from Galactic emission. The directions in these bins are also strongly correlated. The 0-5 bin is not shown in the bottom panel because it is almost identical to the 5-10 bin but (as indicated in the top panel) the vectors are approximately five times longer. The absence of this spectral and directional behavior for the bins 10-15 and larger is evidence that the Galaxy is no longer the major contributor to the directional uncertainty of the dipole. Although the 20-25 bin seems indicative of the spectral behavior of Galactic emission, the incoherent directional behavior is inconsistent with a common spatial origin for the supposed source.

Supporting evidence is provided by the small differences between the dipole solutions using the "custom" cut (Kogut *et al.* 1996b, Fig.1) and the straight $|b| > 20^\circ$ cut presented here. The differences in amplitude, longitude and latitude are less than $0.2\%, 9\%$, and 6% of our error bars on these respective quantities. If plotted in Figure 1, the "custom" cut solutions overlap the $|b| > 20^\circ$ points with a barely distinguishable displacement in the direction of the $|b| > 25^\circ$ solutions.

4.2. Higher Multipole CMB Contamination

For the purposes of determining the dipole there are two sources of noise; instrument noise with a power law spectral index $n \approx 3$ and the $n \approx 1$ CMB signal. At 10° scales the CMB signal to noise ratio in the maps is ~ 1 (Bennett *et al.* 1996). Thus on larger scales the CMB signal dominates the instrument noise and correspondingly, the uncertainties on the dipole from the CMB signal are larger than those from the instrument noise. The uncertainties from *both* are reduced by lowering the Galactic plane cut. In the 15-20 bin of Figure 2 (and to a lesser extent in the 10-15 and 25-30 bins) we see a directional and spectral behavior consistent with a common spatial origin and a CMB spectra (no frequency dependence of the angular deviation). This suggests that large scale power of the CMB signal is responsible for these displacements (rather than Galactic emission), and that a smaller (not a larger) cut is called for. This is further supported by the fact that for $|b| \gtrsim 20^\circ$, the combined free-free and dust emission from the Galaxy at 53 and 90 GHz produces only $\sim 10\,\mu$K rms while the CMB signal rms is $\sim 30\,\mu$K (Bennett *et al.* 1996).

To estimate the uncertainty in the dipole results due to the CMB signal we simulate $n = 1.2$, $Q_{rms-PS} = 15.3\,\mu$K CMB skies for $2 \leq \ell \leq 25$. We superimpose these maps on a known dipole and solve for the dipole using a 15° Galactic plane cut. No bias is detected and the rms's of the results around the input values are $3.3\,\mu$K in amplitude, $0^\circ.076$ in longitude and $0^\circ.053$ in latitude. We include these uncertainties in the combined systematics.

Galactic cuts greater than 15° are not useful corrections which eliminate more and more Galactic contamination; they introduce systematic errors associated with large Galactic cuts due to the increasingly non-orthogonal basis functions $Y_{\ell m}(\theta, \phi)$, over the increasingly limited and thus noisier input data. We conclude that, for the method used here, the Galactic cuts of 10° and 15° are the best compromise to minimize both the effect of the Galaxy and of the systematic uncertainties. The high precision of our dipole direction results depend on this conclusion. Note that this choice for the optimal Galactic cut is smaller than the $\approx 20^\circ$ cut used when one is trying to compute the correlation function or determine the $\ell \geq 2$ components of the power spectrum of the CMB signal which are smaller than the dipole by a factor of ~ 200. For such determinations, the similar compromise for simultaneously minimizing Galactic contamination, instrument noise and other procedural/systematic effects demands a larger cut.

Our results are averages of the 10° and 15° cuts. We adopt the difference between these two solutions as the one σ uncertainty related to this Galactic plane cut choice. We include this uncertainty in the combined systematics, along with the error associated with the aliasing of the CMB signal and the method difference errors mentioned earlier.

5. Summary

The accuracy of the determination of the CMB dipole has been increasing steadily since its first detections. The uncertainties in both the direction and amplitude have been reduced by more than a factor of 10. We have used the DMR four-year data set to obtain a best-fit CMB dipole amplitude 3.357 ± 0.023 mK in the direction $(\ell, b) = (264^\circ.33 \pm 0^\circ.13, +48^\circ.05 \pm 0^\circ.09)$. The uncertainty in the amplitude is dominated by the absolute calibration uncertainty. This is easily seen in Figure 1 by comparing the large error bars on our final result (far right) with the noise-only error bars on the channel results. The directional uncertainty is predominantly due to the combined systematic

REFERENCES

Bennett, C. L., *et al.* 1994, *Ap.J.* , 436, 423

Bennett, C. L., *et al.* 1996, *Ap.J.* , submitted

Fixsen, D. J. *et al.* 1994, *Ap.J.* , 420, 445

Fixsen, D. J. *et al.* 1996, *Ap.J.* , submitted

Kogut, A. *et al.* 1993, *Ap.J.* , 419, 1

Kogut, A. *et al.* 1996a, *Ap.J.* , submitted

Kogut, A. *et al.* 1996b, *Ap.J.* , submitted

Lineweaver, C. L., *et al.* 1995, Astrophysical Letters and Comm.

Partridge, R. B., 1995, *3K: The Cosmic Microwave Background Radiation*, Cambridge Univ. Press:Cambridge, 1995, p.158

Smoot, G. F., *et al.* 1991, *Ap.J.* , 371, L1

Wright, E. L., *et al.* 1994, *Ap.J.* , 420, 1

This preprint was prepared with the AAS LaTeX macros v3.0.

effects discussed above. The DMR dipole results are internally consistent indicating that the statistical error bars given are appropriate; no evidence of unknown channel dependent systematic errors is seen.

Figure 3 contains the main results of this paper and compares them with other *COBE* results: the DMR first year (Kogut *et al.* 1993), the DMR first two years (Bennett *et al.* 1994), a pixel-based likelihood analysis of the four year data (Bennett *et al.* 1996), and the FIRAS (Fixsen *et al.* 1994, Fixsen *et al.* 1996) dipole results. The DMR dipole results and the FIRAS dipole results are seen to be in good agreement; further evidence that the limits of the different systematic uncertainties of these two *COBE* instruments are fairly well understood.

We gratefully acknowledge the many people responsible for the high quality of the *COBE* DMR data. C.H.L. acknowledges support from the French Ministère Affaires Etrangères. L.T. was partially supported by grant DGICYT PB94-0364.

Captions

Figure 1

Amplitudes and Directions of the CMB Dipole. The top panel displays dipole amplitudes from the six independent DMR channels for six different Galactic plane cuts (from left to right, $|b| > 0°$, 5°, 10°, 15°, 20°, 25°, 30°). The error bars are noise only. For each cut, the weighted average over channels is shown on the right. The bottom panel shows the directions of the same dipoles and are denoted with the same point type and size as in the top panel. The channel labels mark the 0° cut solutions (i.e., *no* Galactic plane cut) with the exception of the 31 GHz labels which indicate the 5° cut solutions. The 0° cut 31 GHz results are off the plot at longitude $\approx 271°$. For each channel, the six Galactic cut solutions are connected by lines (31:long dashes, 53:dots, 90:short dashes, average:solid). The direction of the Galactic Center points to higher latitudes for the same reason that one flies north-west from London to arrive at New York. The latitude and longitude ranges were chosen to display an approximately square piece of the sky. For each channel, the direction error bars on the 15° Galactic cut solutions are shown. Our final dipole amplitude, including the calibration uncertainty is the point in the far right of the top panel. The grey box in the bottom panel denotes the 68% confidence levels of our final dipole direction.

Figure 2

Spectral Analysis of the Angular Deviations of the Dipole. The vectors of the angular separations between the points in Figure 1 are indicated here in the bottom panel while their sizes are plotted in the top panel. The A and B channels at each frequency, 31.5, 53 and 90, have been averaged and are represented respectively by triangles, squares, circles (top) and by thin, medium and thick lines (bottom). In the bottom panel, for ease of comparison, the three vectors in a given bin originate at the same point. The 0-5 bin is not shown because it is similar to the 5-10 bin and the vectors are approximately five times longer. In the top panel, the two reference lines originating on the 31 GHz point of the 0-5 and 5-10 bins indicate the expected spectral behavior if the Galactic emission is pure synchrotron (thin) and pure free-free(thick). The points chosen as the common origin of the vectors for each bin are the directions of the channel averages at the smaller of the cuts in each bin pair. The origin latitudes have been offset by 0.18° with respect to each other to avoid confusion.

Figure 3

COBE Dipoles. The DMR dipole results: "1YR": (Kogut *et al.* 1993), "2YR": (Bennett *et al.* 1994), "4YRBen": (Bennett *et al.* 1996), and "4YRLin": (this work:), are consistent with each other and with the FIRAS results (Fixsen *et al.* 1994, 1996).

Table I: **Channel Dipole Results**

Channel	Amplitude (μK)[a]	Galactic Longitude (degrees)	Galactic Latitude (degrees)
31A			
Mean...............	3366	264.50	47.83
Total Error.........	85	0.19	0.22
Noise...............	7	0.14	0.09
Calibration[b]...	84	0.00	0.00
Combined Systematics	10	0.13	0.20
31B			
Mean...............	3358	264.49	47.99
Total Error.........	77	0.28	0.23
Noise...............	9	0.23	0.12
Calibration.........	77	0.00	0.00
Combined Systematics	4	0.17	0.20
53A			
Mean...............	3355	264.33	48.04
Total Error.........	23	0.15	0.10
Noise...............	2	0.07	0.03
Calibration.........	23	0.00	0.00
Combined Systematics	4	0.13	0.09
53B			
Mean...............	3359	264.28	48.08
Total Error.........	24	0.13	0.07
Noise...............	2	0.08	0.04
Calibration.........	23	0.00	0.00
Combined Systematics	4	0.10	0.06
90A			
Mean...............	3359	264.29	48.06
Total Error.........	67	0.17	0.11
Noise...............	4	0.13	0.07
Calibration.........	67	0.00	0.00
Combined Systematics	3	0.12	0.08
90B			
Mean...............	3358	264.28	48.05
Total Error.........	43	0.14	0.08
Noise...............	3	0.10	0.05
Calibration.........	43	0.00	0.00
Combined Systematics	3	0.10	0.06
Total			
Mean...............	3357	264.33	48.05
Total Error.........	23	0.13	0.09
Noise...............	1	0.04	0.02
Calibration.........	23	0.00	0.00
Combined Systematics	4	0.13	0.09

[a] Values are in thermodynamic temperature transformed from antenna temperature by $\Delta T = \Delta T_{ant}(e^x - 1)^2/x^2 e^x$ where $x = h\nu/kT_o$, $T_o = 2.73$K. The conversion factors are thus 1.026, 1.074 and 1.227 for 31.5, 53 and 90 GHz respectively.

[b] see Kogut *et al.* 1996a, Table 2 for absolute calibration uncertainties.

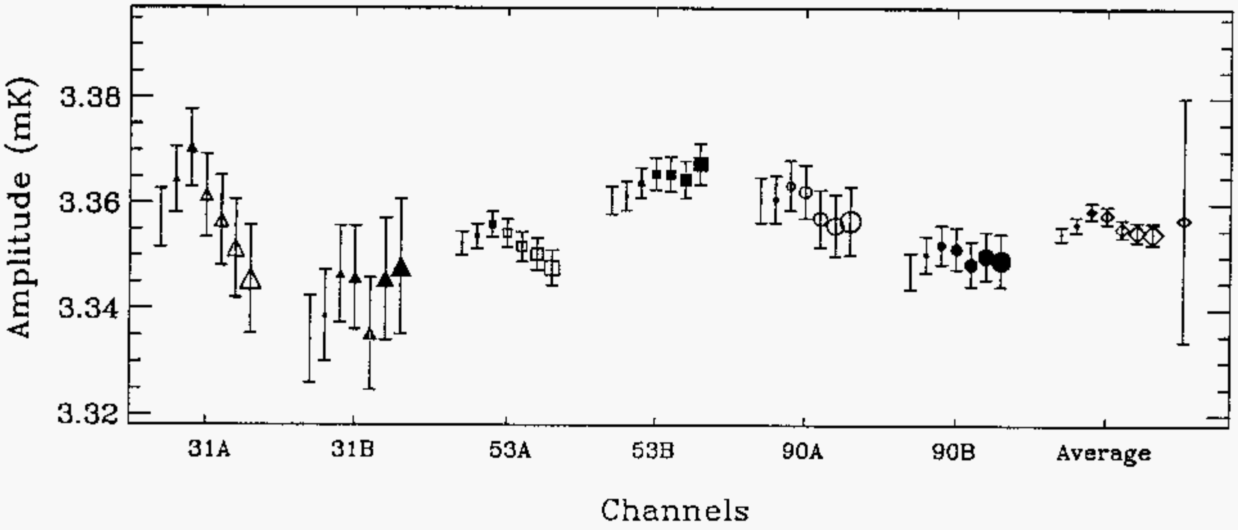
Amplitude (mK)
3.38
3.36
3.34
3.32
31A
31B
53A
53B
90A
90B
Average
Channels

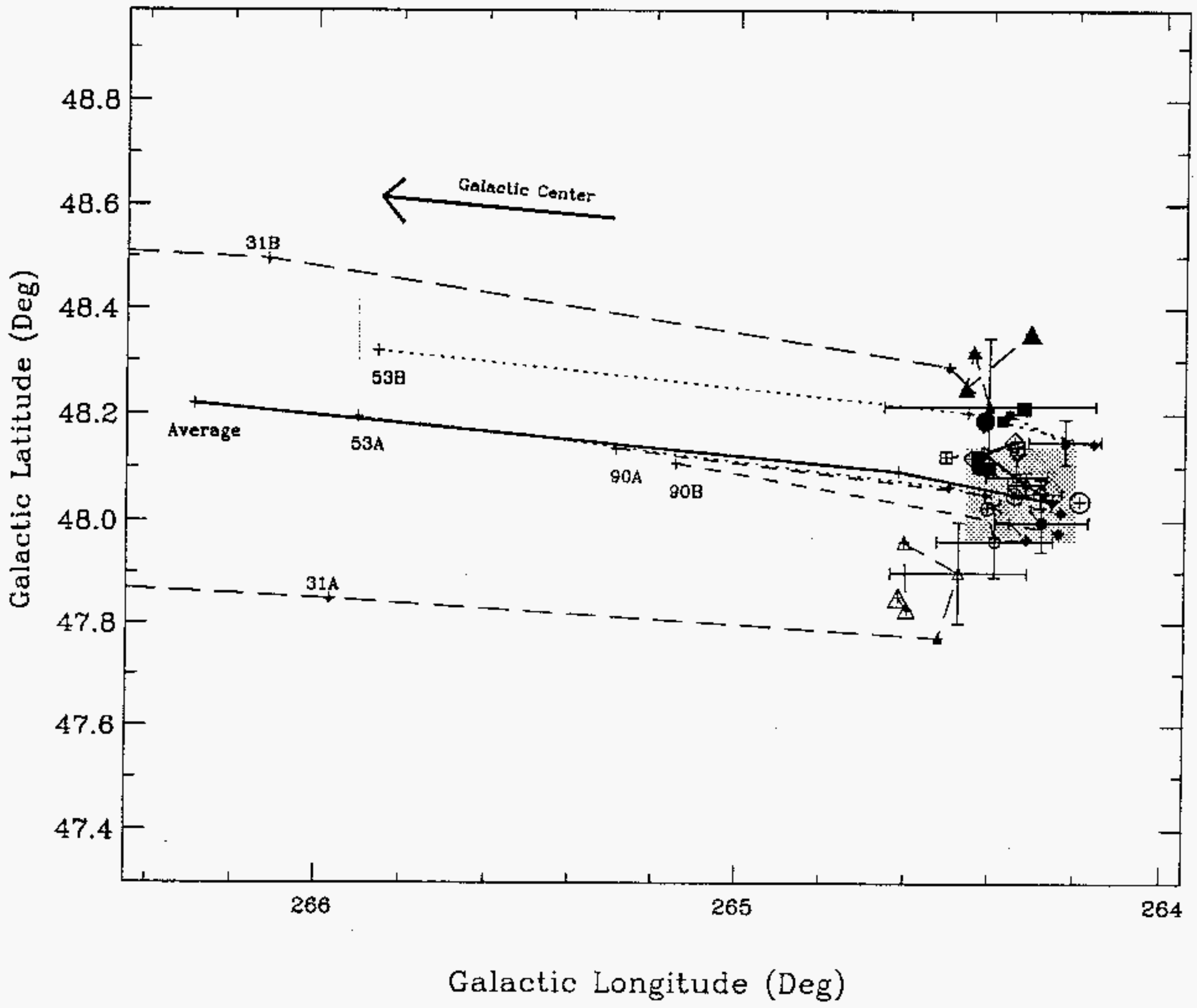
Galactic Center
31B
53B
Average
53A
90A
90B
31A
Galactic Latitude (Deg)
48.8
48.6
48.4
48.2
48.0
47.8
47.6
47.4
266
265
264
Galactic Longitude (Deg)

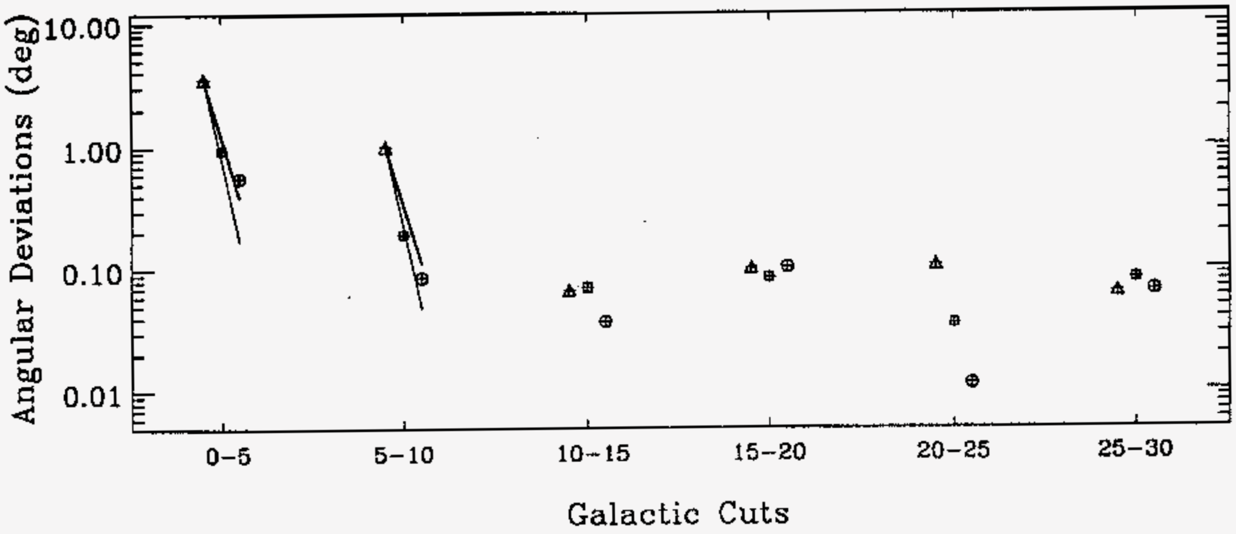
Angular Deviations (deg)
10.00
1.00
0.10
0.01
0-5
5-10
10-15
15-20
20-25
25-30
Galactic Cuts

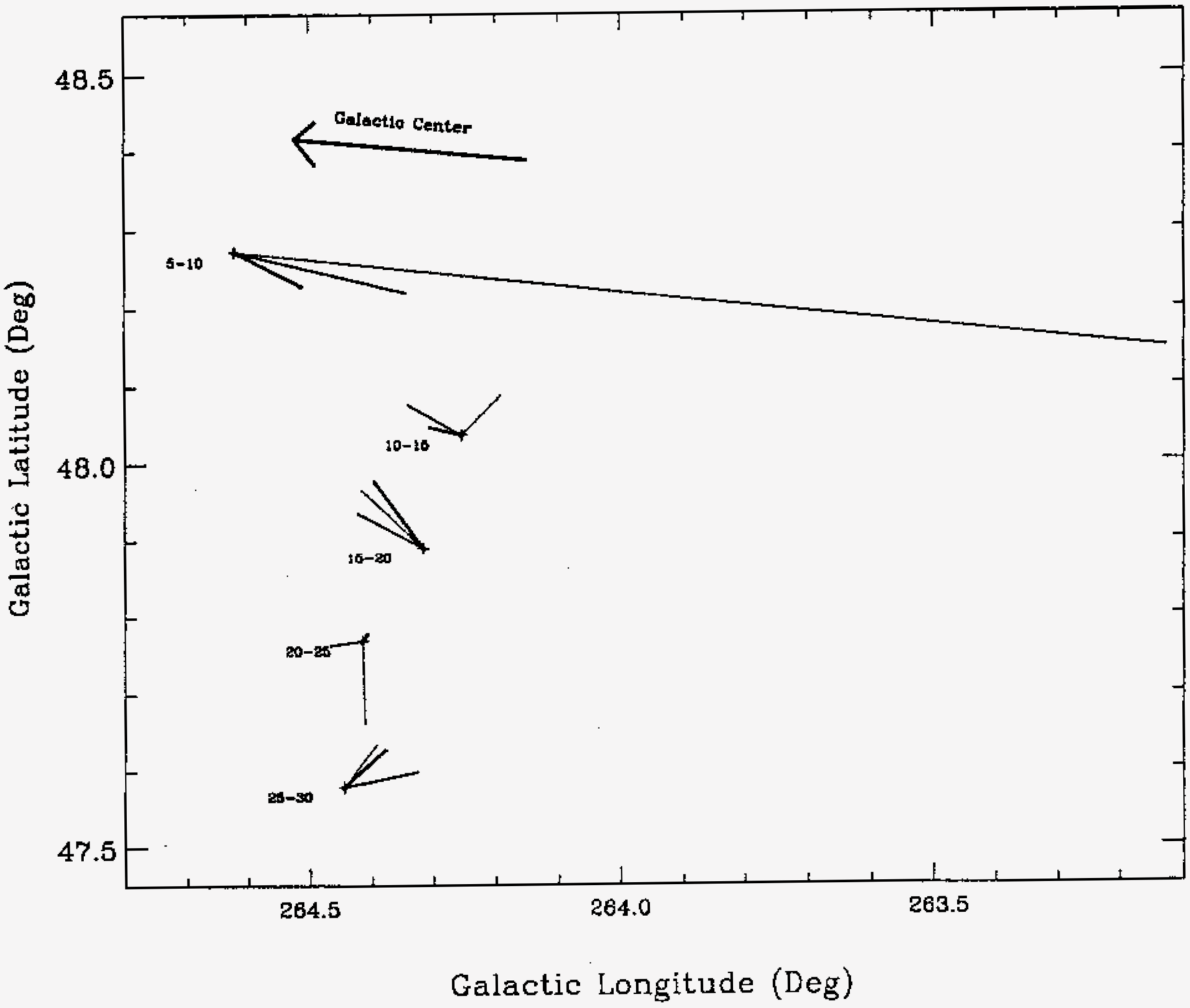
Galactic Latitude (Deg)
48.5
48.0
47.5
Galactic Center
5-10
10-15
15-20
20-25
25-30
264.5
264.0
263.5
Galactic Longitude (Deg)